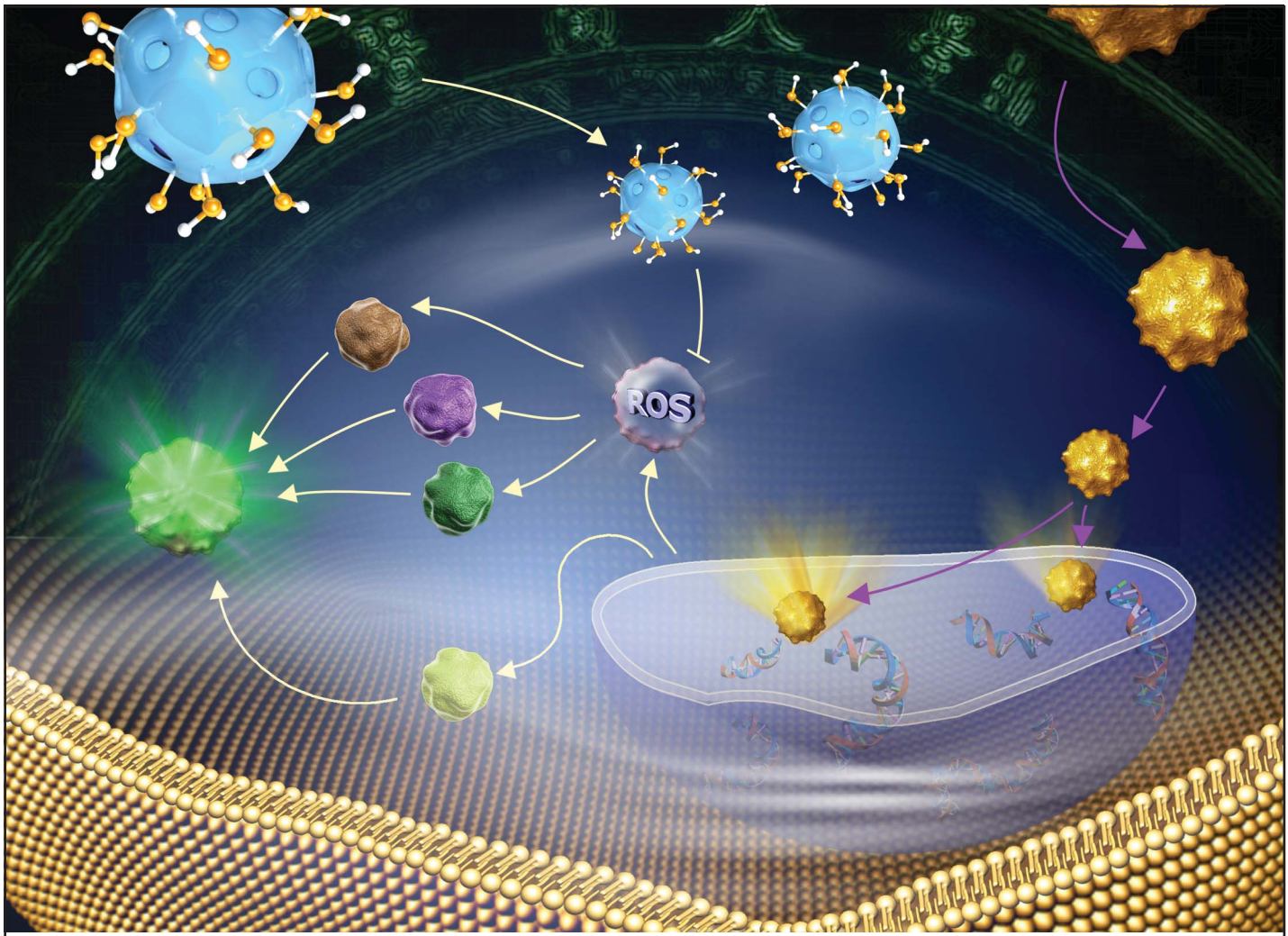

Highlighting research from Prof Tianfeng Chen's group at the Department of Chemistry, Jinan University, China.

Title: Functionalized selenium nanoparticles with nephroprotective activity, the important roles of ROS-mediated signaling pathways

Size controllable and highly stable SeNPs have been designed and prepared by using trolox as a capping agent, which display enhanced antioxidant activity and could suppress cisplatin-induced nephrotoxicity by regulating ROS-mediated signaling pathways.

As featured in:

See Y. Li *et al.*,
J. Mater. Chem. B, 2013, **1**, 6365.

RSC Publishing

www.rsc.org/MaterialsB

Registered Charity Number 207890

Journal of Materials Chemistry B

RSC Publishing

PAPER

View Article Online
View Journal | View Issue

Cite this: J. Mater. Chem. B, 2013, 1, 6365

Functionalized selenium nanoparticles with nephroprotective activity, the important roles of ROS-mediated signaling pathways

Yinghua Li, Xiaoling Li,* Wenjie Zheng, Cundong Fan, Yibo Zhang and Tianfeng Chen*

Received 20th August 2013
Accepted 30th September 2013

DOI: 10.1039/c3tb21168a

www.rsc.org/MaterialsB

The most frequent adverse effect of cisplatin-based chemotherapy is nephrotoxicity. Oxidative stress has been implicated as an important mechanism in the pathogenesis of cisplatin-induced nephrotoxicity. In the present study, 6-hydroxy-2,5,7,8-tetramethylchroman-2-carboxylic acid (trolox) surface-functionalized selenium nanoparticles (Se@Trolox) with enhanced antioxidant activity have been prepared by self-assembly of trolox on the surface of the nanoparticles, and their nephroprotective effects have been investigated. Functionalization by trolox significantly enhanced cell uptake and *in vitro* antioxidant activities of the nanoparticles. In addition, pretreatment with Se@Trolox dose-dependently blocked cisplatin-induced cell growth inhibition against HK-2 cells. Mechanistic investigation suggested that Se@Trolox markedly prevented cisplatin-induced apoptosis in HK-2 cells, as evidenced by inhibition of chromatin condensation, DNA fragmentation, PARP cleavage and activation of caspase-3. Furthermore, Se@Trolox effectively blocked the cisplatin-induced reactive oxygen species (ROS) accumulation, activation of AKT and MAPK signaling and DNA damage-mediated p53 phosphorylation in HK-2 cells. Taken together, our findings suggest that Se@Trolox is a promising Se species with potential application in prevention of cisplatin-induced renal injury.

1 Introduction

Trolox is a water-soluble analogue of α-tocopherol with a chroman ring but lacks a hydrophobic phytyl tail, where the side chain in α-tocopherol is replaced by a more hydrophilic carboxyl group.[1] The antioxidant activity of trolox was proved to be better than that of α-tocopherol under a wide range of conditions and test systems compared with those of several food grade antioxidants.[2] Trolox has been investigated for its protective effects against oxidative stress-related ailments as one of the major phenolic compounds[3] *i.e.* atherosclerosis,[4] global cerebral ischemia[5] and neurodegenerative disorder.[6] E. Soheili Majd *et al.* showed that trolox significantly reduced the cytotoxicity of resin-based biomaterials but had no effect on GIC and RM-GIC biomaterials.[7] Although it has potent antioxidant function and an important role in clinical treatment, it shows low utilization due to its poor aqueous solubility and inferior stability when exposed to an oxygen-containing environment owing to the phenolic hydroxyl group of trolox.[8,9]

Cisplatin (*cis*-diamminedichloroplatinum(II)) is one of the oldest available chemotherapeutic drugs that has been used for the treatment of a wide spectrum of solid tumors, including testicular, ovarian, esophageal, bladder, head and neck cancer and non-small cell lung cancers since the 1960s.[10–12] The chemotherapeutic action of cisplatin is to cross-link with DNA, thereby interfering with transcription and/or DNA replication in tumor cells.[13] Although cisplatin has shown remarkable efficacy at attacking various tumors, it has been found that 65–98% of the platinum is bound to proteins in blood within 24 h of intravenous injection of cisplatin, and the platination of proteins may contribute to severe side effects, attributing to the indiscriminate accumulation of the drug in both normal and cancerous tissues, which leads to acute renal failure.[14–16] In renal proximal tubules, cisplatin causes intrastrand and interstrand crosslinking between N^7 and O^6 of the adjacent guanine molecules, which results in local denaturation of the DNA.[17] Although the molecular mechanism is not completely understood, reactive oxygen species (ROS) have been suggested to be as important mediators of cisplatin-induced nephrotoxicity.[18] Lee and Ajith showed the protective effect of antioxidants against cisplatin-induced nephrotoxicity.[19,20] Therefore, the goal of our work is to attempt to introduce nanotechnology into the development of trolox to protect the kidney from cisplatin-induced injury.

The essential micronutrient selenium (Se) plays a fundamental role in humans and animals and has been implicated to have important health benefits. In humans, selenium has one of the narrowest ranges between dietary deficiency (<40 μg per day) and toxic levels (>400 μg per day). The dietary reference

Department of Chemistry, Jinan University, Guangzhou 510632, China. E-mail: tchentf@jnu.edu.cn; fenling03@gmail.com

value of Se intake has been set in the range of 30–55 μg per day by international agencies.[21] Selenium at supranutritional levels has been shown as a cancer preventive agent in reducing the incidence of colon, prostate, and lung cancer.[22] Studies showed that the dose, chemical form and metabolic activity are the determinants of anticancer activities of Se compounds.[23] Se displayed a narrow margin between the beneficial and toxic effects. As an anticancer agent, the effective dose of Se is close to the toxic range, which greatly limits its clinical application. Although regarded as an essential trace element, Se is toxic if taken in excess.[24] Selenocompounds act as an essential component of several major metabolic pathways, including thyroid hormone metabolism, antioxidant defense systems and in trolox function.[25] Se nanoparticles (SeNPs) attract increasing attention due to their excellent anticancer activities and low toxicity.[26] We have previously demonstrated that surface decoration of SeNPs with polysaccharide and sialic acids significantly enhanced the antiproliferative activities of SeNPs.[27] Our previous work has demonstrated that selenium nanoparticles by self-assembly of 11-mercapto-1-undecanol (Se@MUN) achieved enhanced antioxidant activity and antagonism against cisplatin-induced nephrotoxicity.[18] But the stability of Se@MUN is poor, so we need to find more stable nanoparticles for future applications.

The combination of nanotechnology, biochemistry, biotechnology and molecular biology has developed into an emerging research area: nanobiotechnology, which offers exciting opportunities for developing new nanosized materials and providing paradigm-breaking solutions in this area because these technologies provide extremely high sensitivity.[28,29] The application of nanotechnology to drug delivery is widely expected to change the landscape of pharmaceutical and biotechnology industries for the foreseeable future. These are a few of the many compelling reasons that nanotechnology holds enormous promise for drug delivery. For example, it may be possible to improve the delivery of poorly water-soluble drugs and deliver drugs in a cell- or tissue-specific manner. Additionally, the manufacturing complexity of nanotechnology therapeutics may also create a significant hurdle for generic drug companies to develop equivalent therapeutics readily.[30] The excellent performance of bionanomaterials opens new horizons for drug delivery and therapy of diseases that have traditionally been recognized as incurable *via* basic therapies or surgical methods.[31] In this study, we hypothesized that the assembly of antioxidant ligands on SeNPs could exert the synergism of Se and the capping agents in scavenging free radicals, and the aim of the present study is to validate this hypothesis and use trolox functionalized SeNPs (Se@Trolox) to antagonize cisplatin-induced nephrotoxicity through scavenging free radicals. Taken together, functionalization of SeNPs by trolox significantly enhanced the ability of Se@Trolox antagonizing cisplatin-induced nephrotoxicity through scavenging ROS in HK-2 cells and regulating the AKT and MAPK pathways.

2 Materials and methods

Materials

Thiazolyl blue tetrazolium bromide (MTT), propidium iodide (PI), 2′,7′-dichlorofluorescein diacetate (DCF-DA), 4′,6-diamidino-2-phenylindole (DAPI), bicinchoninic acid (BCA) kit and Na_2SeO_3 were purchased from Sigma-Aldrich chemicals. Terminal transferase dUTP nick end labeling (TUNEL) assay kit was obtained from Roche Applied Science (Basel, Switzerland). Caspase-3 substrate (Ac-DEVD-AMC) was purchased from Biomol (Germany). Caspase-9 substrate (Ac-LEHD-AFC) and caspase-8 substrate (Ac-IETD-AFC) were purchased from Biomol (Germany). Dulbecco's modified Eagle's medium (DMEM) and fetal bovine serum (FBS) were purchased from Gibco BRL (Gaithersburg, MD). Vitamin C was purchased from Guangzhou chemical reagent factory. The water used in all experiments was Milli-Q water.

Preparation of Se@Trolox: synthesis of Trolox–SH

Trolox (0.5 g) was mixed with cystamine dihydrochloride (0.11 g), benzotriazol-1-yloxytris (dimethylamino) phosphonium hexafluorophosphate (BOP), 0.39 g, 1-hydroxy-1*H*-benzotriazole, monohydrate (HOBt) 0.134 g, and 4-(dimethylamino) pyridine (DMAP) 0.108 g in dry *N*,*N*-dimethylformamide (DMF) (10 ml). After a brief activation period (10 min), *N*-methylmorpholine (0.9 g) was added to the reaction mixture and the solution was stirred under N_2 at room temperature for 18 h. Solvent was removed under vacuum, and the residue was dissolved in ethyl acetate, then washed with 0.5 M H_2SO_4, 1 M Na_2CO_3, and brine, each for three times. The organic layer was dried over anhydrous $MgSO_4$, and the solvent was evaporated *in vacuo*. The residue was separated by column chromatography on silica gel to purify (Trolox–S)$_2$. The reduction of (Trolox–S)$_2$ by sodium borohydride in ethanol yielded the thiol ligand Trolox–SH.

Synthesis of Trolox–SH functionalized SeNPs (Se@Trolox)

Briefly, 0.5 ml of 50 mM vitamin C solution was added dropwise into 62.5 ml of 0.1 M Na_2SeO_3 solution under magnetic stirring, and the mixture was reconstituted to a final volume of 25 ml with Milli-Q water. Then the mixed solution was stirred for half an hour at room temperature. When the colour of the solution completely became red, the pH was adjusted to 10 with 0.1 M NaOH. After that, 3.86 mg of Trolox–SH powder dissolved in 1 ml absolute ethyl alcohol was added under magnetic stirring overnight at room temperature. The color turned grey subsequently, and the nanoparticles were centrifuged at 10 000 × *g* for 30 min and washed with Milli-Q water and absolute ethyl alcohol each for three times. Finally, the solution was subjected to centrifugation at 8000 rpm for 15 min and freeze-dried. Se@Trolox powder was stored at −20 °C until use. To determine the cellular uptake of Se@Trolox, the nanoparticles containing a fluorescent dye 6-coumarin were prepared using a similar procedure except that 100 mg of the dye was added to the reaction system after the addition of trolox. The incorporated dye acts as a probe for Se@Trolox and offers a sensitive method to determine their intracellular uptake and localization.

Characterization of Se@Trolox

The as-prepared products were characterized by using various methods. Briefly, TEM samples were prepared by dispersing the

powder particles onto a holey carbon film on copper grids. The micrographs were obtained on a Hitachi (H-7650) for TEM operating at an accelerating voltage of 80 kV. EDX analysis was carried out on an EX-250 System (Horiba) and employed to examine the elemental composition of Se@Trolox. FT-IR samples were recorded on an Equinox 55 IR spectrometer in the range of 4000–500 cm^{-1} using the KBr-disk method.

ABTS free radical scavenging assay

ABTS free radical scavenging activities of Se@Trolox were measured as previously described.[32]

Cell culture and cell viability assay

HK-2 proximal tubular cell line derived from the normal human kidney was purchased from American Type Culture Collection (ATCC, Manassas, VA) and grown in DMEM medium, supplemented with 10% fetal bovine serum (FBS), 100 units per ml penicillin and 50 units per ml streptomycin in a humidified incubator at 37 °C with a 5% CO_2 atmosphere. Cell viability was determined by measuring the ability of cells to transform MTT to a purple formazan dye as previously described.[33]

In vitro cellular uptake of Se@Trolox

The cellular uptake of Se@Trolox was also monitored qualitatively by fluorescence microscopy.[31] Briefly, treated cells cultured on a cover glass in 6-well plates till 70% confluence were incubated with different concentrations of 6-coumarin-loaded Se@Trolox for various periods of time. The cells were then washed three times with PBS and examined under a fluorescence microscope (AMG EVOS f1). For quantitative analysis of cellular uptake, Se concentrations in the cells after treatments were determined by the ICP-MS method.[34]

Localization and uptake pathways of Se@Trolox

The intracellular localization of coumarin-6-loaded Se@Trolox in HK-2 cells was traced with the lysosomal marker Lyso Tracker Red as previously described.[35] Briefly, the treated cells cultured on a cover glass in 6-well plates to 70% confluence were incubated with 6-coumarin-loaded Se@Trolox and Lyso Tracker Red at 37 °C for various periods of time. Then the stained cells were rinsed three times with PBS and examined under a fluorescence microscope.

Flow cytometric analysis

Cell cycle distribution was monitored by flow cytometric analysis as previously described.[36] The proportion of cells in G0/G1, S, G2/M phases was represented as a DNA histogram. Apoptotic cells with hypodiploid DNA content were measured by quantifying the sub-G1 peak in the cell cycle pattern. For each experiment 10 000 events per sample were recorded.

TUNEL assay and DAPI staining

DNA fragmentation was examined by fluorescence staining with the TUNEL apoptosis detection kit according to the manufacturer's instructions.[37]

Determination of activities of caspase-3, -8 and -9

The caspase activities in the cells exposed to cisplatin and Se@Trolox were determined by using specific caspase-3, -8, and -9 substrates.[38]

Measurement of ROS generation

Intracellular ROS accumulation was evaluated by DCF fluorescence assay. Briefly, cells were harvested and suspended in PBS (1×10^6 cells per ml) containing 10 mM of DCFH-DA. After incubation at 37 °C for 30 min, the stained cells were collected and resuspended in PBS. Then, the ROS level was determined by measuring the fluorescence intensity using a microplate reader, with the excitation and emission wavelengths set at 500 and 529 nm respectively. Experiments were performed in triplicate.

Western blotting

The effects of cisplatin on the expression levels of various intracellular proteins in HK-2 cells and the protection of Se@Trolox were examined by Western blot analysis as previously described.[23] The bands were visualized with enhanced chemiluminescence reagent that detects the target proteins on the X-ray film.

Statistical analysis

All the data are presented as mean ± SD. Differences between two groups were evaluated using two-tailed Student's *t* test. One-way analysis of variance[39] was used in multiple group comparisons. These analyses were carried out using SPSS 13.0. Difference with $P < 0.05$ (*) or $P < 0.01$ (**) was considered statistically significant.

3 Results and discussion

Preparation and characterization of Se@Trolox

In this study, we demonstrated a simple method to synthesize functionalized SeNPs through self-assembly of functional ligands on the surface of nanoparticles. SeNPs were capped with trolox molecules to form more compact and stable globular

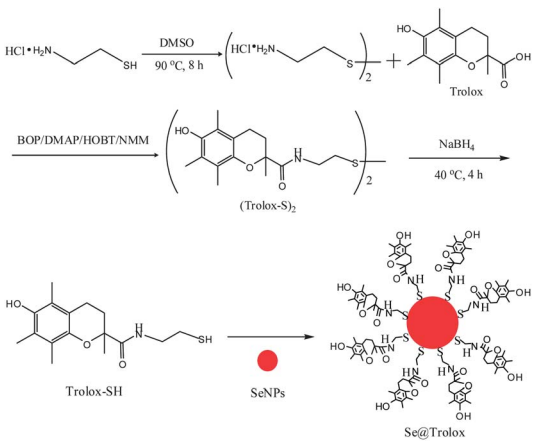

Scheme 1 Synthetic route towards Se@Trolox.

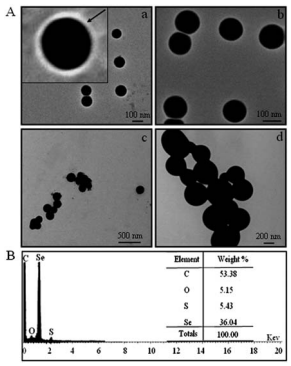

Fig. 1 (A) TEM images of Se@Trolox (a and b) and SeNPS (c and d). (B) EDX analysis of Se@Trolox.

nanocomposites (Scheme 1). The morphology and chemical composition of Se@Trolox were characterized using various spectroscopic and microscopic methods. Fig. 1A shows the TEM images of the SeNPs with the presence (a and b) and absence (c and d) of the capping agent trolox, which clearly demonstrated that Se@Trolox presented a monodisperse and homogeneous spherical structure with an average diameter of about 100 nm, whereas SeNPs in aqueous solutions easily aggregated and precipitated. Fig. 1B, an elemental composition analysis employing EDX showed the presence of a strong signal from the Se atoms (36.04%), together with a S atom signal (5.43%), C (53.38%) and O (5.15%) from trolox. The presence of an S atom indicates that trolox was self-assembled on the surface of Se@Trolox. Se@Trolox was further characterized by FTIR to confirm the chemical binding of trolox to the surface of the nanoparticles. As shown in Fig. 2A, the FTIR spectrum of Se@Trolox resembles that of trolox, giving clear evidence that this antioxidant ligand forms part of the nanocomposite. The absence of an S–H peak at 2580 cm^{-1} stretching mode in the IR spectrum of Se@Trolox indicates the formation of the thiolate–Se bond between the ligands and the SeNP surface. Stability is an important issue for the nanoparticles' future applications.[40]

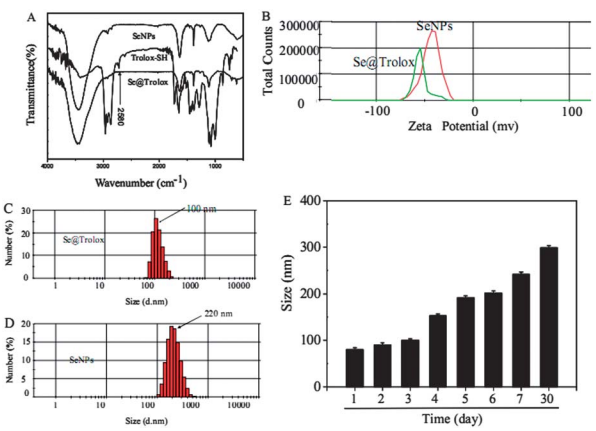

Fig. 2 (A) The FT-IR of Se@Trolox. (B) Zeta potential of Se@Trolox and SeNPs. (C) and (D) Size distribution of Se@Trolox and SeNPs. (E) Stability of Se@Trolox in aqueous solutions.

To examine the effects of trolox on the surface properties and stability of SeNPs, we measured the zeta potential and size distribution of SeNPs and Se@Trolox. As shown in Fig. 2B, the zeta potential of Se@Trolox was lower than SeNPs after trolox surface decoration, explaining the higher stability of Se@Trolox than SeNPs. Fig. 2C and D show that the average particle size of Se@Trolox was effectively decreased from 220 nm to about 100 nm. Furthermore, in Fig. 2E, we used a Zetasizer Nano-ZS particle analyzer to test the changes in the size distribution of Se@Trolox in aqueous solutions. The results revealed that Se@Trolox remained stable at least for 30 days in aqueous solutions.

Cellular uptake of Se@Trolox

Cellular uptake is an important factor that usually contributes to nanomaterial-based drug cytotoxicity. In the present study, a quantitative analysis of cellular uptake was conducted by ICP-MS.

HK-2 cells were incubated with different concentrations of nanoparticles and then subjected to acidic digestion and ICP-MS analysis. As shown in Fig. 3A, HK-2 cells treated with 5, 10, 20 and 40 μg ml^{-1} Se@Trolox displayed a dose-dependent increase in Se cellular uptake, which was significantly higher than those of Se@MUN and SeNPs alone. The dramatic increase in cellular uptake of SeNPs could be due to the enhancement of endocytosis, one of the most important entry mechanisms for extracellular nanomaterials.[31] Taken together, these results suggest that trolox surface decoration enhances the cellular uptake of SeNPs.

Localization and uptake pathways of Se@Trolox

Endocytosis is an important uptake pathway for nanoparticles.[41] In this study, the localization of Se@Trolox in HK-2

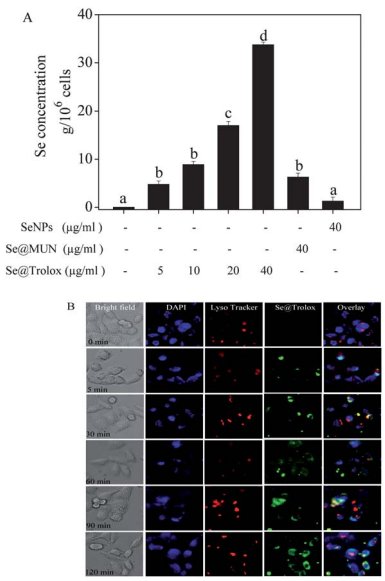

Fig. 3 (A) Quantitative analysis of Se concentrations by ICP-MS and (B) localization and uptake pathways of Se@Trolox.

cells was investigated by using specific probes, Lyso Tracker Red and DAPI, for fluorescence imaging of lysosomes and cell nucleus, respectively. As shown in Fig. 3B, the combination of blue, red, and green fluorescence clearly indicates the colocalization of Se@Trolox and lysosomes in HK-2 cells after 5 min, which increased in a time-dependent manner. Se@Trolox escaped from lysosomes after 15 min and then released into the cytosol and distributed in cells after 60 min. During the whole process, the fluorescence from Se@Trolox could not be observed in the nucleus. These results suggest that lysosomes are the main target organelles of Se@Trolox.

Se@Trolox suppresses cisplatin-induced cytotoxicity

Several studies have demonstrated the protective effect of antioxidants on kidneys against cisplatin-induced nephrotoxicity.[42] Therefore, treatment with antioxidants could be an effective way to ameliorate this damage. Our previous studies have found that trolox is a thiol-containing functional ligand with antioxidant activity.[43] The present study aimed at evaluating the nephrotoxicity protective effect of trolox-functionalized SeNPs against cisplatin-induced acute renal damage. Firstly, we examined the cytotoxicity of cisplatin on HK-2 cells and protective effects of Se@Trolox by using MTT reduction assay. As shown in Fig. 4A, HK-2 cells treated with 8 μg ml^{-1} of cisplatin for 24 h showed a cell viability of 31.25% However, the cytotoxicity was significantly attenuated by Se@Trolox in a dose-dependent manner. For instance, at concentrations 10 and 20 μg ml^{-1}, Se@Trolox increased the cell viability to 85.3 and 90.2% of control, which were significantly higher than those of free trolox and Se@MUN under the same concentrations. Cells treated with 40 μg ml^{-1} of Se@Trolox alone showed no difference in cell viability from those of control cells. These results suggest that organized and ordered assembly of trolox on the surface of nanoparticles effectively amplified the nephroprotective activity of SeNPs. The protective effects of Se@Trolox were confirmed by phase-contrast observation. As shown in Fig. 4B, cells treated with cisplatin showed cytoplasmic shrinkage, reduction in cell numbers and loss of cell-to-cell contact. These cisplatin-induced morphological changes were attenuated by co-treatment with Se@Trolox. By contrast, control cells and cells treated with Se@Trolox alone appeared healthy, with regularity in shape and well developed cell-to-cell contact. These results indicated that Se@Trolox was able to attenuate cisplatin-induced nephrotoxicity.

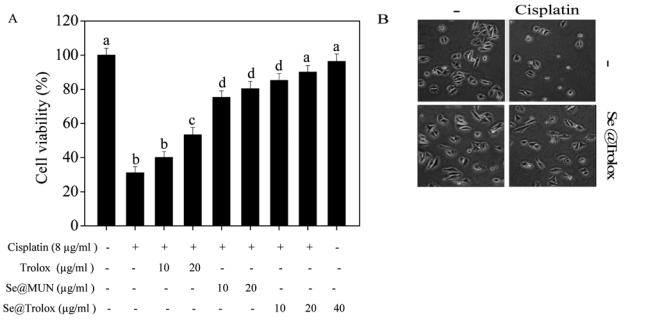

Fig. 4 Se@Trolox rescues HK-2 cells from cisplatin-induced cytotoxicity. (A) Cells were pretreated with Se@Trolox or SeNPs for 12 h and then exposed to 8 μg ml^{-1} cisplatin for 24 h. Cell viability was measured by MTT assay. (B) Morphological changes in HK-2 cells were observed by phase-contrast microscopy.

Blocking of cisplatin-induced apoptosis by Se@Trolox

Apoptosis or programmed cell death is an essential process of cell death during embryonic and postnatal tissue remodeling and some other pathological conditions, such as nephrotoxicity caused by cisplatin. In the present study, flow cytometry was used to evaluate the degree of apoptotic cell death caused by cisplatin. As shown in Fig. 5A, the apoptotic cells with DNA fragmentation show a typical sub-G1 peak in the DNA histogram. For instance, 8 μg ml^{-1} of cisplatin reduced the cell viability of 30%. However, the sub-G1 apoptotic cell population was significantly decreased by co-treatment with Se@Trolox in a dose-dependent manner. At concentrations of 10 and 20 μg ml^{-1}, Se@Trolox reduced the apoptotic cells to 12% and 12.8%, respectively. Se@Trolox alone did not exhibit apoptosis-inducing effect on HK-2 cells. The protection of Se@Trolox against cell apoptosis was further confirmed by TUNEL enzymatic labeling and DAPI co-staining assay. DNA fragmentation is an important biochemical hallmark of cell apoptosis. TUNEL assay can be used to detect early stage of DNA fragmentation in apoptotic cells prior to the changes in morphology. As shown in Fig. 5B, after treatment with 8 μg ml^{-1} cisplatin, HK-2 cells exhibited typical apoptotic features, such as DNA fragmentation (green fluorescence) and nuclear condensation (blue fluorescence). A significant increase in the number of TUNEL-positive

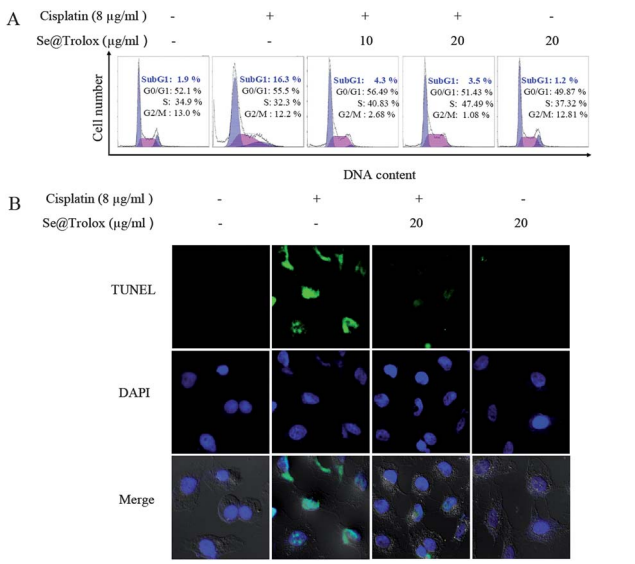

Fig. 5 Se@Trolox blocks cisplatin-induced apoptosis in HK-2 cells. (A) Apoptotic cell population was determined by PI flow cytometric analysis. (B) Representative photomicrographs of DNA fragmentation and nuclear condensation as detected by TUNEL-DAPI co-staining assay. Cells were pretreated with Se@Trolox or SeNPs for 12 h and then exposed to 8 μg ml^{-1} cisplatin for 24 h. All results were representative of three independent experiments. Cells were pretreated with Se@Trolox for 12 h and then exposed to 8 mg ml^{-1} cisplatin for 24 h. All results were representative of three independent experiments.

cells and the fluorescence intensity were observed after 24 h treatment with cisplatin. However, co-treatment with Se@Trolox effectively blocked the cisplatin-induced DNA fragmentation and changes in nuclear morphology. The number of TUNEL-positive cells was significantly decreased in cisplatin-treated HK-2 cells. Moreover, cells exposed to Se@Trolox alone showed normal nuclei of oval shape, similar to those of the control cells. These results indicate that Se@Trolox rescues HK-2 cells from cisplatin-induced nephrotoxicity through blocking of cell apoptosis.

Se@Trolox suppresses cisplatin-induced caspase activation

The caspase family of aspartate-specific cysteine proteases plays important roles in the initiation and execution of apoptosis.[44] Among them, caspase-3 has been regarded as the central regulator of apoptosis, while caspase-8 and -9 act as initiators of death receptor-mediated and mitochondria-mediated apoptotic pathways, respectively. In this study, to determine whether caspase family was activated in HK-2 cells exposed to cisplatin, the enzymatic activities of caspase-3,-8 and -9 were measured by using specific substrates. The results (Fig. 6A and B) show that treatments of the cells with 20 μg ml^{-1} of Se@Trolox significantly suppressed the activation of caspase-3,-8 and -9 induced by cisplatin, demonstrating that Se@Trolox protects HK-2 cells from cisplation-induced injury through death receptor-mediated and mitochondria-mediated pathway inhibition of caspase activation.

Se@Trolox inhibits cisplatin-induced ROS generation

ROS consists of highly reactive molecules, including oxygen ions, free radicals, and peroxides. Oxidative stress refers to a situation of a marked imbalance between cellular defense mechanisms and ROS production. ROS is generated as a natural by product of normal cellular metabolism and has important roles in cell signaling. ROS has been proposed to involve in the initiation phase of apoptosis contributing to cell death signaling.[45] Several lines of evidence have demonstrated that cisplatin-induced renal failure was accompanied by ROS production and peroxidative damage.[46] In this study, we showed that cisplatin significantly increased the intracellular ROS generation in HK-2 cells to 390% of the control group (Fig. 7A). Interestingly, we found that Se@Trolox significantly inhibited cisplatin-induced ROS generation in a dose-dependent manner. For instance, at concentrations of 10 and 20 μg ml^{-1}, Se@Trolox reduced the intracellular ROS to 350% and 310%, respectively. Our results indicate that Se@Trolox is capable of scavenging free radicals and protecting HK-2 cells against cisplatin-induced oxidative stress.

Antioxidant activity of Se@Trolox

The total antioxidant activity of Se@Trolox was determined by using ABTS free radical scavenging assay. In this system, the relatively long-lived $ABTS^{+}$ generated by the direct oxidation of ABTS with manganese dioxide is decolorized during the reaction with hydrogen-donating antioxidants.[47] This assay provides a direct comparison of the antioxidant activities of tested samples as expressed in terms of absorbance. As shown in Fig. 7B, Se@Trolox significantly inhibited the formation of ABTS free radicals in a time-and dose-dependent manner, which was higher than those of free trolox and Se@MUN. These results support the enhancement of the antioxidant activity of SeNPs by trolox surface decoration. Based on these results, the strategy to assemble antioxidant ligands on the surface of SeNPs

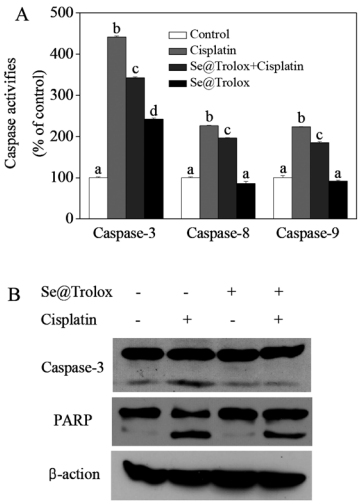

Fig. 6 Inhibition of caspase activation by Se@Trolox. (A) Cells were pretreated with or without Se@Trolox for 12 h and then cultured in the presence or absence of 8 μg ml^{-1} cisplatin for 24 h. Caspase activity was measured with whole cell extracts by a fluorometric method. All data are expressed as means ± SD from three independent experiments, each performed in duplicate. Bars with different characters are statistically different at $P < 0.05$ level. (B) Induction of caspase-3 and PARP cleavage by cisplatin and the protective effects of Se@Trolox.

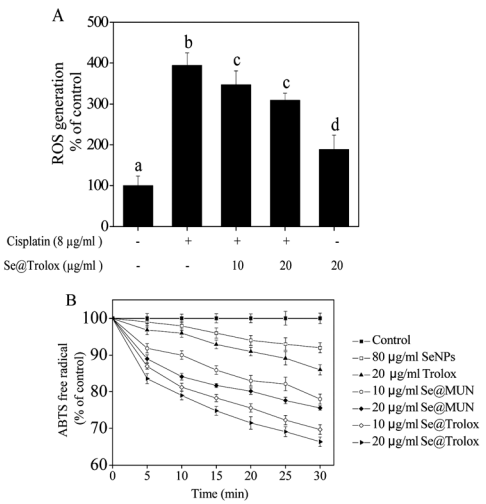

Fig. 7 Se@Trolox blocks cisplatin-induced ROS generation by scavenging free radicals. (A) Cells were pretreated with Se@Trolox for 12 h and then cultured in the presence of 8 μg ml^{-1} cisplatin for 24 h. Intracellular ROS generation was determined by DCFH-DA assay and expressed as a percentage of control cells. All data are expressed as means ± SD from three independent experiments, each performed in duplicate. Bars with different characters are statistically different at $P < 0.05$ level. (B) Antioxidant activities of Se@Trolox as determined by ABTS assay.

could be a highly efficient way to enhance the antioxidant activity.

Se@Trolox blocks various cisplatin-induced signaling pathways

As shown in Fig. 8A, we proposed the signaling pathways accounting for the nephroprotective effects of Se@Trolox. AKT is a stress-sensitive kinase regulated by the intracellular redox system.[48] The status of ROS has been found to play an important role in the regulation of the AKT signaling pathway.[39] Once activated, AKT can inhibit apoptosis by a number of actions, including phosphorylation and inhibition of proapoptotic Bcl-2 family members, GSK3β, and forkhead family transcription factors.[49] In this study, Western blot analysis was used to examine the effects of Se@Trolox on the expression and phosphorylation level of AKT in HK-2 cells. As shown in Fig. 8B, Se@Trolox treatment led to an obvious decrease in total and phosphorylated AKT in HK-2 cells in a dose-dependent manner, suggesting that Se@Trolox induces cancer cell apoptosis through inhibition of the AKT pathway. MAPK signaling pathways have also been found to play important roles in the action of chemotherapeutics and are suggested to participate in various cellular processes, including cell proliferation, differentiation and apoptosis. MAPKs can be activated by a variety of stimuli including growth factors, hormones, mitogens, and stress factors. Oxidative stress is a key modulator of MAPK signaling cascades.[50] In this study, Western blot analysis was used to examine the involvement of MAPK pathway Se@Trolox-induced apoptosis.

It was found that Se@Trolox treatment triggered a differential response of JNK ERK and p38 MAPK in HK-2 cells (Fig. 8C). A significant decrease in total and phosphorylated ERK was observed in cells exposed to Se@Trolox. A slight increase in p-JNK and p38 was also detected in the treated cells, while the expression of total JNK remained constant. These results suggest that MAPK pathways were involved in cancer cell apoptosis induced by Se@Trolox. The role of the p53 signaling pathway is one of the most common genetic alterations identified in human tumors and many chemotherapeutic drugs result in either DNA damage or microtubule inhibition. The action of p53 as a tumor suppressor protein has been elucidated through the discovery and analysis of downstream target genes. Therefore, the biochemical characterization of p53 could also give us a glimpse of how p53 regulates cell physiology.[51] As shown in Fig. 8D, Se@Trolox treatment moderately decreased the expression of total p53 protein.

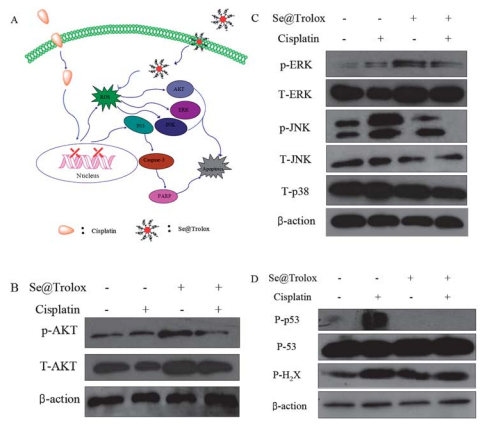

Fig. 8 Se@Trolox blocks cisplatin-induced signaling pathways. (A) Proposed signaling pathways accounting for the nephroprotective effects of Se@Trolox. (B) Effects of Se@Trolox on the phosphorylation status and expression level of AKT. (C) Effects of Se@Trolox on the phosphorylation status and expression level of MAPKs in cells exposed to cisplatin. (D) Effects of Se@Trolox on DNA damage-mediated p53 phosphorylation in HK-2 cells.

4 Conclusions

In summary, we present a strategy to use trolox as a capping agent for preparation of size controllable and highly stable SeNPs with enhanced antioxidant activity and antagonism against cisplatin-induced nephrotoxicity. The studies on the underlying mechanisms revealed that Se@Trolox blocked the caspase-mediated apoptosis induced by cisplatin through inhibition of ROS mediated p53 phosphorylation. Furthermore, Se@Trolox effectively protects HK-2 cells from cisplatin-induced injury by regulating the AKT and MAPK pathways. Taken together, our findings suggest that Se@Trolox is a promising Se species with potential application in prevention of cisplatin-induced renal injury.

Acknowledgements

This work was supported by National Science and Technology Support Program (2012BAC07B05), Science Foundation for Distinguished Young Scholars of Guangdong Province, Natural Science Foundation of China and Guangdong Province, Program for New Century Excellent Talents in University, Research Fund for the Doctoral Program of Higher Education of China and China Postdoctoral Science Foundation.

Notes and references

1 J. B. Arellano, H. Li, S. Gonzalez-Perez, J. Gutierrez, T. B. Melo, F. Vacha and K. R. Naqvi, *Biochemistry*, 2011, **50**, 8291–8301.
2 R. R. Yettella and D. B. Min, *J. Agric. Food Chem.*, 2008, **56**, 10887–10892.
3 L. Han, L. B. Du, A. Kumar, H. Y. Jia, X. J. Liang, Q. Tian, G. J. Nie and Y. Liu, *Biomaterials*, 2012, **33**, 8517–8528.
4 N. Abudu, J. J. Miller and S. S. Levinson, *Free Radical Res.*, 2006, **40**, 321–331.
5 S. Gupta and S. S. Sharma, *Biol. Pharm. Bull.*, 2006, **29**, 957–961.
6 M. L. da Frota Junior, A. S. Pires, F. Zeidan-Chulia, I. J. Bristot, F. M. Lopes, M. A. de Bittencourt Pasquali, A. Zanotto-Filho, G. A. Behr, F. Klamt, D. P. Gelain and J. C. Moreira, *Mol. Cell. Biochem.*, 2011, **358**, 325–334.
7 E. S. Majd, M. Goldberg and L. Stanislawski, *Biomaterials*, 2003, **24**, 3–9.
8 Y. I. Li, G. Elmer and R. C. LeBoeuf, *Life Sci.*, 2008, **83**, 557–562.

9 D. S. Fagundes, S. Gonzalo, M. P. Arruebo, M. A. Plaza and M. D. Murillo, *Dig. Liver Dis.*, 2010, **42**, 40–44.
10 D. W. Shen, L. M. Pouliot, J. P. Gillet, W. T. Ma, A. C. Johnson, M. D. Hall and M. M. Gottesman, *Mol. Pharmaceutics*, 2012, **9**, 1822–1833.
11 L. Banci, I. Bertini, O. Blazevits, V. Calderone, F. Cantini, J. F. Mao, A. Trapananti, M. Vieru, I. Amori, M. Cozzolino and M. T. Carri, *J. Am. Chem. Soc.*, 2012, **134**, 7009–7014.
12 X. H. Peng, Y. Q. Wang, D. H. Huang, Y. X. Wang, H. J. Shin, Z. J. Chen, M. B. Spewak, H. Mao, X. Wang, Y. Wang, Z. Chen, S. M. Nie and D. M. Shin, *ACS Nano*, 2011, **5**, 9480–9493.
13 X. Xue, S. You, Q. Zhang, Y. Wu, G. Z. Zou, P. C. Wang, Y. L. Zhao, Y. Xu, L. Jia, X. N. Zhang and X. J. Liang, *Mol. Pharmaceutics*, 2012, **9**, 634–644.
14 C. T. Wu, M. L. Sheu, K. S. Tsai, C. K. Chiang and S. H. Liu, *Free Radical Biol. Med.*, 2011, **51**, 671–680.
15 N. B. Zhang, Y. G. Du, M. Cui, J. P. Xing, Z. Q. Liu and S. Y. Liu, *Anal. Chem.*, 2012, **84**, 6206–6212.
16 G. E. Craig, S. D. Brown, D. A. Lamprou, D. Graham and N. J. Wheate, *Inorg. Chem.*, 2012, **51**, 3490–3497.
17 Y. Sanchez-Perez, R. Morales-Barcenas, C. M. Garcia-Cuellar, R. Lopez-Marure, M. Calderon-Oliver, J. Pedraza-Chaverri and Y. I. Chirino, *Chem.-Biol. Interact.*, 2010, **188**, 144–150.
18 Y. H. Li, X. L. Li, Y. S. Wong, T. F. Chen, H. B. Zhang, C. R. Liu and W. J. Zheng, *Biomaterials*, 2011, **32**, 9068–9076.
19 J. H. Lee, H. J. Lee, H. J. Lee, W. C. Choi, S. W. Yoon, S. G. Ko, K. S. Ahn, S. H. Choi, K. S. Ahn, J. C. Lieske and S. H. Kim, *Phytomedicine*, 2009, **16**, 188–197.
20 T. A. Ajith, V. Nivitha and S. Usha, *Food Chem. Toxicol.*, 2007, **45**, 921–927.
21 L. H. E. Winkel, C. A. Johnson, M. Lenz, T. Grundl, O. X. Leupin, M. Amini and L. Charlet, *Environ. Sci. Technol.*, 2012, **46**, 571–579.
22 S. J. Ramos, Y. X. Yuan, V. Faquin, L. R. G. Guilherme and L. Li, *J. Agric. Food Chem.*, 2011, **59**, 3657–3665.
23 T. F. Chen and Y. S. Wong, *Int. J. Biochem. Cell Biol.*, 2009, **41**, 666–676.
24 W. Liu, X. L. Li, Y. S. Wong, W. J. Zheng, Y. B. Zhang, W. Q. Cao and T. F. Chen, *ACS Nano*, 2012, **6**, 6578–6591.
25 H. B. Zhang, T. F. Chen, J. Jiang, Y. S. Wong, F. Yang and W. J. Zheng, *J. Agric. Food Chem.*, 2011, **59**, 8683–8690.
26 H. L. Wang, J. S. Zhang and H. Q. Yu, *Free Radical Biol. Med.*, 2007, **42**, 1524–1533.
27 T. Chen, Y. S. Wong, W. Zheng, Y. Bai and L. Huang, *Colloids Surf., B*, 2008, **67**, 26–31.
28 M. Magro, A. Faralli, D. Baratella, I. Bertipaglia, S. Giannetti, G. Salviulo, R. Zboril and F. Vianello, *Langmuir*, 2012, **28**, 15392–15401.
29 M. T. Martinez, Y. C. Tseng, M. Gonzalez and J. Bokor, *J. Phys. Chem. C*, 2012, **116**, 22579–22586.
30 O. C. Farokhzad and R. Langer, *ACS Nano*, 2009, **3**, 16–20.
31 Y. Mi, Y. T. Liu and S. S. Feng, *Biomaterials*, 2011, **32**, 4058–4066.
32 T. F. Chen and Y. S. Wong, *J. Agric. Food Chem.*, 2008, **56**, 4352–4358.
33 J. S. Zheng, S. Y. Zheng, Y. B. Zhang, B. Yu, W. J. Zheng, F. Yang and T. F. Chen, *Colloids Surf., B*, 2011, **83**, 183–187.
34 Y. Y. Huang, L. Z. He, W. Liu, C. D. Fan, W. J. Zheng, Y. S. Wong and T. F. Chen, *Biomaterials*, 2013, **34**, 7106–7116.
35 W. Li, L. N. Zhao, T. T. Wei, Y. L. Zhao and C. Y. Chen, *Biomaterials*, 2011, **32**, 4030–4041.
36 X. L. Li, T. F. Chen, Y. S. Wong, G. Xu, R. R. Fan, H. L. Zhao and J. C. N. Chan, *Int. J. Biochem. Cell Biol.*, 2011, **43**, 525–534.
37 T. F. Chen, Y. A. Liu, W. J. Zheng, J. Liu and Y. S. Wong, *Inorg. Chem.*, 2010, **49**, 6366–6368.
38 H. L. Wu, X. L. Li, W. Liu, T. F. Chen, Y. H. Li, W. J. Zheng, C. W. Y. Man, M. K. Wong and K. H. Wong, *J. Mater. Chem.*, 2012, **22**, 9602–9610.
39 C. Huang, J. Li, M. Ding, S. S. Leonard, L. Wang, V. Castranova, V. Vallyathan and X. Shi, *J. Biol. Chem.*, 2001, **276**, 40234–40240.
40 Q. Li, T. F. Chen, F. Yang, J. Liu and W. J. Zheng, *Mater. Lett.*, 2010, **64**, 614–617.
41 F. Wang, Y. C. Wang, S. Dou, M. H. Xiong, T. M. Sun and J. Wang, *ACS Nano*, 2011, **5**, 3679–3692.
42 R. Cetin, E. Devrim, B. Kilicoglu, A. Avci, O. Candir and I. Durak, *J. Appl. Toxicol.*, 2006, **26**, 42–46.
43 Z. Nie, K. J. Liu, C. J. Zhong, L. F. Wang, Y. Yang, Q. Tian and Y. Liu, *Free Radical Biol. Med.*, 2007, **43**, 1243–1254.
44 R. Sinha and K. Ei-Bayoumy, *Curr. Cancer Drug Targets*, 2004, **4**, 13–28.
45 M. Czarna and W. Jarmuszkiewicz, *Postepy Biochem.*, 2006, **52**, 145–156.
46 C. A. Davis, H. S. Nick and A. Agarwal, *J. Am. Soc. Nephrol.*, 2001, **12**, 2683–2690.
47 L. P. Leong and G. Shui, *Food Chem.*, 2002, **76**, 69–75.
48 Y. C. Ou, C. R. Yang, C. L. Cheng, S. L. Raung, Y. Y. Hung and C. J. Chen, *Eur. J. Pharmacol.*, 2007, **563**, 49–60.
49 L. del Peso, M. Gonzalez-Garcia, C. Page, R. Herrera and G. Nunez, *Science*, 1997, **278**, 687–689.
50 X. L. Li, G. Xu, T. F. Chen, Y. S. Wong, H. L. Zhao, R. R. Fan, X. M. Gu, P. C. Y. Tong and J. C. N. Chan, *Int. J. Biochem. Cell Biol.*, 2009, **41**, 1526–1535.
51 Z. A. Stewart and J. A. Pietenpol, *Chem. Res. Toxicol.*, 2001, **14**, 243–263.

